

INVESTIGATIONS OF PROTRACTED FINNED DOUBLE PIPE HEAT EXCHANGER SYSTEM FOR WASTE HEAT RECOVERY FROM DIESEL ENGINE EXHAUST

by

Srinath SOUNDARARAJAN^{a*} and Mahalingam SELVARAJ^b

^a Department of Mechanical Engineering,

Vidyaa Vikas College of Engineering and Technology, Namakkal, India

^b Department of Mechanical Engineering, Sona College of Technology, Salem, India

Original scientific paper

<https://doi.org/10.2298/TSCI230212143S>

The need for energy and material savings, as well as environmental concerns, have helped to increase the demand for high efficiency heat exchangers in the modern era. In practice, a heat exchanger or the direct ejection of the hot working fluid is used to recover the waste heat from a heat engine or thermal power plant into the environment. Waste heat of a heat engine or power plant is recovered to the environment via a heat exchanger or by direct ejection from the hot working fluid. In many situations, waste heat recovery removes or greatly reduces the necessity for additional fuel energy input to achieve this goal. The double pipe heat exchanger equipment is taken in this research, heat from engine exhaust recovers due to its superior qualities. The design characteristics of the heat pipe will be changed in order to increase overall efficiency by studying the concepts of various authors. Different design parameters for a double pipe heat exchange system as well as different working fluid-flow rates are tested with the suggested device. Additionally, ANSYS performs CFD for the proposed heat exchanger system in order for the results to support the experimental findings.

Key words: engine exhaust gas, heat transfer, thermal efficiency, ANSYS-CFD, double pipe heat exchanger, waste heat recovery system

Introduction

Considering their lifespan, high thermal efficiency, and low maintenance requirements, Diesel engines are frequently employed in cars and small-scale power generation. Most of the remaining fuel energy is lost by internal combustion engines (ICE) through heat losses, exhaust gas, and exhaust gas re-circulation. Within ICE, 30-45% of the fuel energy is transformed to labour output [1]. The rate of heat transfer aimed at heat exchanger with baffles is boosted by looking at the thermal analysis results. When baffles are utilised, the displacement and stresses are lower than for a heat exchanger without one [2]. When working with nanofluid coolants, a thorough optimization design approach is necessary since several factors relating to the design of the heat exchanger and nanofluid itself might impact the efficiency of the heat recovery method. The volume percentage of the nanoparticles has a considerable impact on the thermophysical properties of the nanofluid as well as the performance of the heat recovery heat exchanger, including the rate of heat transfer and tube side pressure-drop [3, 4]. The efficiencies fluctuate significantly across various air coolers and intercoolers by around 20%, which results

* Corresponding author, e-mail: ssrinathmech@outlook.com

in an increase in energy recovery rate of roughly 3%. The enhancement of energy recovery requires the use of a more efficient heat exchanger [5, 6]. The shell and tube method is found to maximise heat extraction from all the heat exchangers and is best suited for recovering waste heat from exhaust gases from vehicles. The effectiveness of the non-optimized, store-bought heat exchangers was discovered to be 0.44, which is much less than a heat exchanger that has been carefully constructed. The efficacy of the heat exchangers was raised to 0.76 after being optimised for this specific application. The best heat exchanger design was found to be capable of recovering 2.9 kW at 15 bar operating pressure at the engine's rated load [7]. The protracted finned counter flow heat exchanger's efficiency may operate at full capacity between 71% and 75% of the time. A heat exchanger with fins of a length of 1 m will have an efficiency that is 10-13% higher than one without. The amount of fins and their length increased, improving the efficiency of the heat recovery and raising brake thermal performance from 32-37% [8].

Various kinds of heat exchangers are utilised to exploit the extra heat energy in exhaust gases, according to the literature review. Previous studies mostly concentrated on recovering thermal energy from exhaust with protracted finned heat exchangers or heat exchangers with different tapes and inserts. However, no studies pertaining to the heat exchanger with novel heat recovery with the combination of twisted tape and protracted finned tube were contacted. For Diesel engines, this entails the creation of new technical system on exhaust heat recovery system to enhance the energy recovery and lower emissions from exhaust. The following are the primary goals of the current study:

- Creating a CFD model using ANSYS to study heat transport in a protracted finned double pipe heat exchanger (PFDPHE).
- To examine the parameters and heat transfer properties of a PFDPHE with various fin configurations.
- Experimentation is done to verify the analytical outcomes of the CFD model.
- Analysing the proposed model's total rate of heat transfer and coefficient of heat transfer in comparison the existing model.

Experimentation set-up

Aditya *et al.* [9], one of the research scholars, provided the geometry of the double pipe, extended finned tube heat exchangers employed in the simulation study. However, the dimensions and fin profile designs were adjusted. In his research, he found that using 12 fins with a 30 mm height of the protrusion resulted in the lowest temperature of exhaust gas outlet and peak heat transfer rate. Figure 1 depicts the experimental configuration schematically while tab. 1 provides geometric specifications. In the current study, three models are examined to prove their performance compared to normal DPHE, fig. 2, 8 fins with a 10 mm protrusion height are taken into consideration and fin geometry are varied as flat fin, fig. 3, fin with horizontal wing cut, fig. 4, and fin with alternate horizontal wing cut, fig. 5. The consequence of fins and tape in DPHE have been investigated and the effect of heat transfer when different fin geometry and number of fins varied have been analysed using ANSYS FLUENT. Both counter-flow and parallel-flow analysis have been done and compared with normal DPHE (which has no fins and tapes for fluid-flow interruptions). Each sample receives a unique experimental and numerical simulation analysis, and the experimentation time is held constant at 10 minutes.

Internal combustion exhaust heat energy is predominantly recovered by the protracted-finned heat exchanger design. The exhaust gas mass-flowrate for a chosen Diesel engine was estimated when listing the heat exchanger designs by combining the mass-flow rates of air and fuel for single cylinder Diesel engines. In order to extract the heat, the working fluid used in

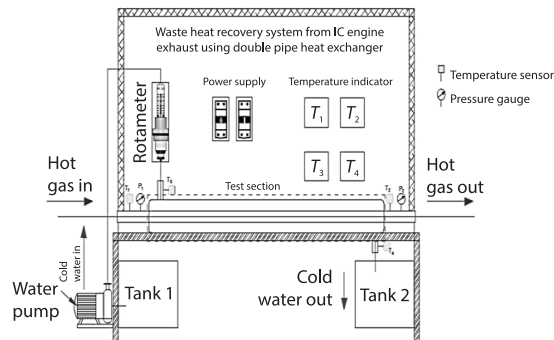


Figure 1. Experiment set-up of PFDPHE for waste heat recovery system

Table 1. Geometry details of DPHE

Parameters	Units	Symbols	Inside	Outside
Inside diameter of pipe	[mm]	d_i, D_i	46.9	73
Outside diameter of pipe	[mm]	d_o, D_o	50	76.2
Total length of pipe	[mm]	L	1000	1000
Thickness of pipe	[mm]	t	1.5	1.5
Protrusion height of fins	[mm]	H_f	10	–
Total length of fins	[mm]	L_f	1000	–
Thickness of fin	[mm]	t_f	3	–

heat exchangers is essential. Table 2 is a list of the characteristics of employed fluids, including water as a cold fluid while engine exhaust gas as a hot fluid. Steel, with a favourable thermal conductivity value of 45 W/mK, is chosen as the heat exchanger material.

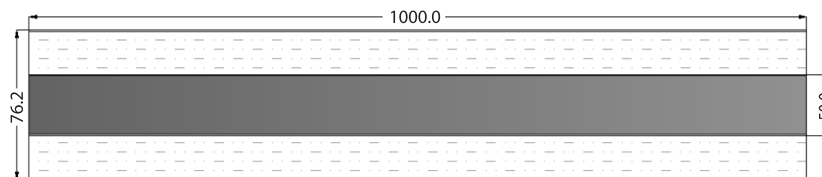


Figure 2. Lay-out of DPHE for waste heat recovery system

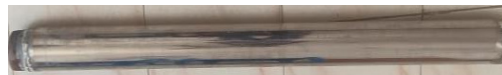
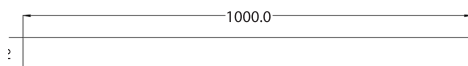


Figure 3. Lay-out of flat fin attached with inside tube

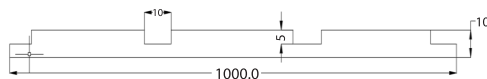
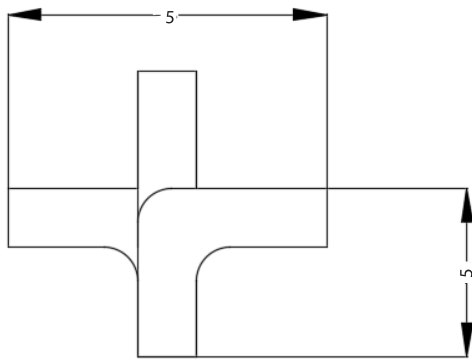


Figure 4. Lay-out of horizontal wing cut fin

Table 2. Hot fluid and cold fluid properties of PFDPE

Input Parameter	Units	Symbols	Hot fluid	Cold fluid
Thermal conductivity	[Wm ⁻¹ K ⁻¹]	K_h, K_c	0.0404	0.6
Specific heat capacity	[Jkg ⁻¹ K ⁻¹]	C_{p_h}, C_{p_c}	1030	4182
Viscosity	[Nsm ⁻²]	μ_h, μ_c	0.000027	0.0006
Density	[kgm ⁻³]	ρ_h, ρ_c	0.696	998
Mass-flow rate	[kgs ⁻¹]	m_h, m_c	0.00934	0.0054

**Figure 5. Cross-section lay-out of alternate horizontal wing cut fin**

A DPHE set-up is fabricated using stainless steel and corresponding geometric specifications used is specified with aforementioned figs. 3-5. The design lay-out of modelled component is shown in fig. 2. The DPHE set-up is taken and evaluated with the proposed design. Proposed design, which having eight number of protracted fins attached on outer side of the inner tube. Fins with and without alternate horizontal wing cut is taken as proposed design. Waste heat recovery and simulation analysis were conducted using 1-cylinder, 4-stroke, water cooled, naturally aspirated Diesel engine. The engine's technical details are listed in tab. 2 of the document. The

mass-flow rate via a sharp edge orifice was precisely measured using a venturi metre to measure air-flow. Using chromel-alumel J -type thermocouple, the temperature of exhaust gas was determined. The extended outside finned counter flow heat exchanger was developed and put into use in a DPHE for recovery of exhaust heat using water as the working fluid based on thermodynamical assessments of exhaust gas temperature at various positions in engine exhaust manifold.

Design data of waste heat recovery heat exchanger

The heat balance equation is utilized to calculation of the temperature of the hot fluid as it exits the heat exchanger, T_{h_2} [10]. Absorbed heat by water = carried heat by exhaust gas:

$$m_w C_{p_w} \Delta t_w = m_c C_{p_c} \Delta t_c \quad (1)$$

For heat exchanger, [11] the effectiveness is determined:

$$\text{Effectiveness} = \left[\frac{T_{h_1} - T_{h_2}}{T_{h_1} - T_{c_2}} \right] \quad (2)$$

For multi-pass heat exchangers, the correction factor must be multiplied by logarithmic mean temperature difference (LMTD) [12]. The LMTD is given:

$$LMTD = \left[\frac{(T_{h_1} - T_{c_1})(T_{h_2} - T_{c_2})}{\log_e \frac{T_{h_1} - T_{c_1}}{T_{h_2} - T_{c_2}}} \right] \quad (3)$$

For the specific design under consideration, the following equation was used to compute the co-efficient of total heat transfer, U , for PFDPHE:

$$\eta_{\text{mean}} = \frac{\eta_{\text{hot}} - \eta_{\text{cold}}}{2} \quad (4)$$

$$\text{Pr} = \frac{\text{molecular diffusivity of moment}}{\text{molecular diffusivity of heat}} \quad (5)$$

$$\text{Re} = \frac{\text{inertia forces}}{\text{viscous forces}} \quad (6)$$

$$\text{Nu} = \frac{hL}{K} \quad (7)$$

where L is the typical length, while K is the fluid's thermal conductivity.

Based on the eqs. (5)-(7):

$$U = \frac{Q_{\text{avg}}}{A_1 \Delta T_{lm}} \quad (8)$$

Result of mass-flowrate and fluid specific heat derived for convection process for experimentation [13, 14]:

$$C = mC_p \quad (9)$$

$$Q = mc\Delta T \quad (10)$$

The total heat transfer rate may be estimated using eqs. (8) and (10). One may precisely determine the entire heat transfer rate and make educated judgements on heat management by using the eqs. (8) and (10), which take into account elements like temperature differences and thermal conductivity.

Finite volume analysis

By ANSYS FLUENT, a number of numerical simulations were run to examine the temperature characteristics, heat transport, and system efficiency of a PFDPHE. By comparing the exhausting gas temperature derived numerically at the PFDPHE output to that of experimental findings, the numerical results are confirmed. Numerical analysis uses the energy balance equation eq. (1) to identify the output temperature. Boundary conditions of 508.15 K for the engine exhaust temperature and 305.15 K for the coolant temperature were employed for the validation efforts. Exhaust gas temperature variations from simulations of three different protracted fin designs [15, 16].

Figures 7-9 shows the 3-D model created using solidworks. Figures 10 and 11 illustrates the model geometry and mesh geometry which imported to ANSYS workbench (FLUENT). Figure 12 shows the FLUENT model with boundary conditions of PFDPHE.

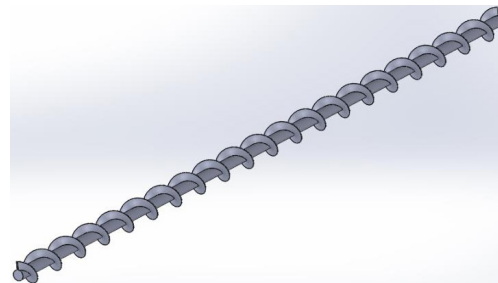


Figure 7. Twisted tape insert model in solid works

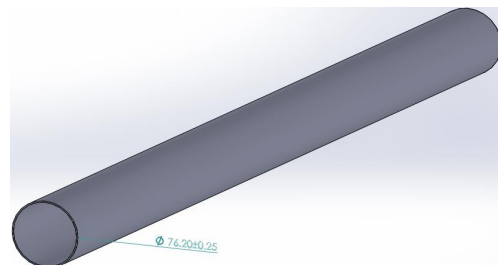


Figure 8. Outer tube model in solid works

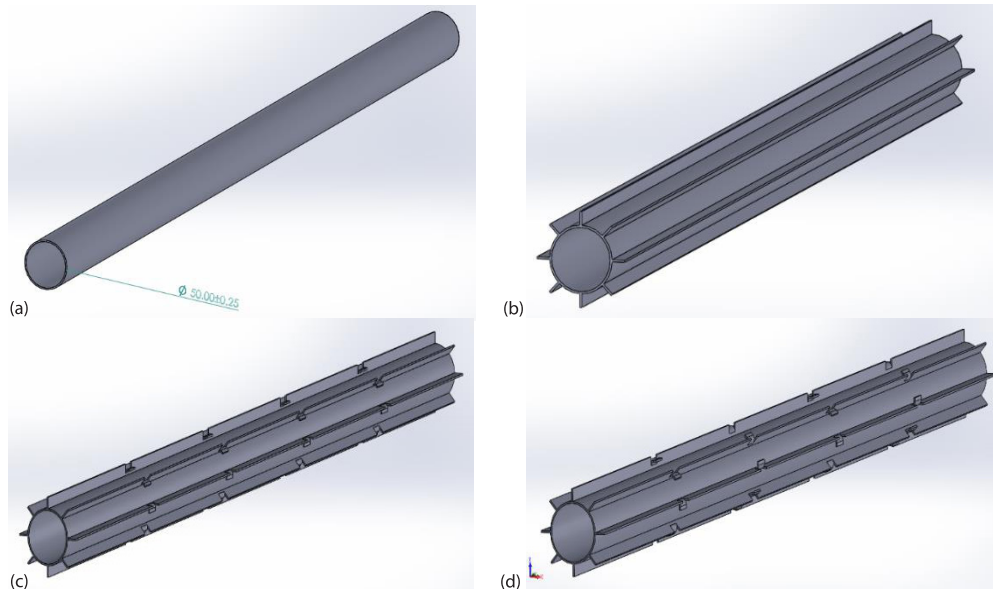


Figure 9. Inner tube model in solid works; (a) normal, (b) with fins, (c) fins with horizontal wing cuts, and (d) fins with alternate horizontal wing cuts

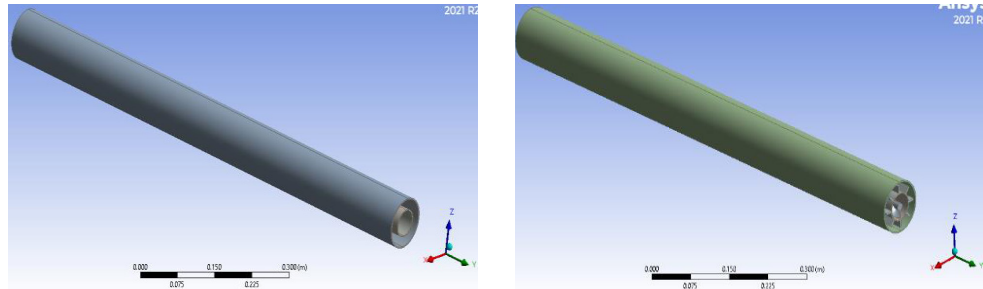


Figure 10. The 3-D model imported in ANSYS

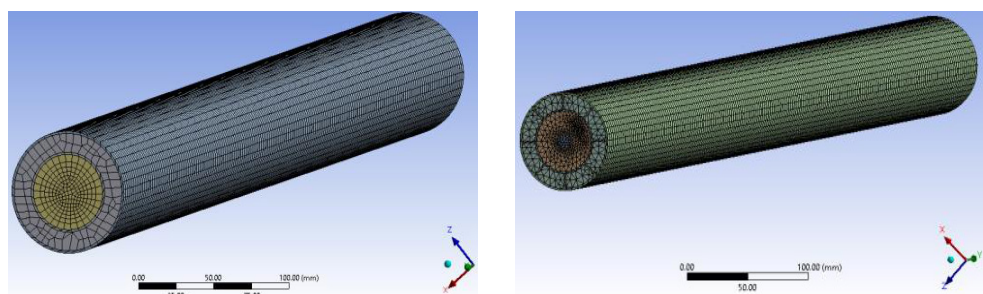


Figure 11. Mesh geometry of normal and protracted finned tube

Appropriate boundary conditions are in place for the discretized flow domain. Inlets were given mass-flow boundary conditions, whereas outputs got pressure outlet boundary conditions. The surfaces of the heat exchangers were observed as regular wall boundaries.

The inner walls had connected thermal wall boundary conditions, whilst the outside walls had insulated boundary characteristics. Laterally with flow and energy equations, the standard $k-\epsilon$ equation is utilised to address the turbulence problem [17]. Tables 2 and 3 summarize, the thermodynamic characteristics and boundary conditions of heat exchanger working fluids.

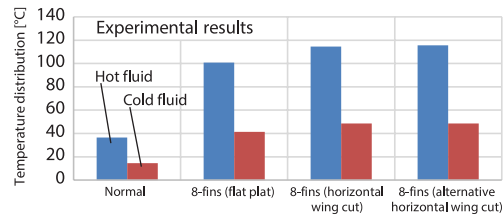


Figure 12. Temperature distribution of experimental results of protracted finned double pipe tube heat exchanger

Table 3. Details of boundary conditions

Details	Boundary type	Value	Units
Inlet-exhaust gas	Mass-flow inlet	0.00934	[kgs ⁻¹]
Inlet-cold water	Mass-flow inlet	0.0054	[kgs ⁻¹]
Inlet temperature of hot fluid	Temperature	508.15	[K]
Inlet temperature of cold fluid	Temperature	305.15	[K]
Outlet	Pressure outlet	0	[Pa]
Inner surfaces, fin surfaces	Standard wall	Coupled	–
Outer surfaces	Standard wall	Heat flux = 0	–
Turbulent model	$k-\epsilon$	Standard	–

Result and discussion

Temperature distribution

Figure 13 displays the distribution of temperature for normal model and the protracted finned tube model of heat exchanger at mass-flowrate of 0.00934 kg/s for exhaust gas and 0.0054 kg/s for cold water. The experiment revealed that the cold-water outlet temperature increased by an average of 287.64 K while the exhaust gas outlet temperature of the heat exchanger model without fins decreased by an average of 309.68 K. The findings show that introducing twisted tape inserts and protracted finned tubes with alternate horizontal wing cuts to the heat exchanger’s inner tube causes the output water temperatures to decrease. This is a result of the heat exchanger’s increased heat transfer area [18, 19]. From the simulation, it was discovered that the exhaust gas temperature (outlet) of the heat exchanger is dropped by 307.23 K and the cold water outlet temperature increases an average value of 559.83 K for those with and fins, respectively.

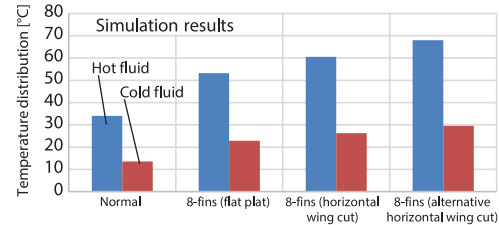


Figure 13. Temperature distribution of simulation results of protracted finned double pipe tube heat exchanger

From figs. 12 and 13, it is found that the heat exchanger with protracted finned tube DPHE yields the best performance amongst others. In fig. 12, experimental values of temperature difference between output temperature values are presented and proved that the 8-fins with an alternate horizontal wing cut (Model 4) are 68.41% and 70.09% better than the normal tube (Model 1) for both hot and cold fluids, respectively. protracted tube (Model 2) with 8-fins is 64.94% and 63.77% times better than the normal tube for both hot and cold fluids. The protracted tube (Model 3) with a horizontal wing cut is 68.14% and 70.11% times better than the normal tube for hot and cold fluids, respectively. Figure 13 shows the simulation results of the

temperature difference between the output temperature values, demonstrating that the 8-fins with an alternate horizontal wing cut (Model 4) outperform the regular tube (Model 1) for both hot and cold fluids, respectively. For both hot and cold fluids, the extended tube (Model 2) with 8-fins outperforms the standard tube by 68.14% and 70.11%, respectively. For hot and cold fluids, the prolonged tube (Model 3) with a horizontal wing cut outperforms the standard tube by 68.14% and 70.11%, respectively. The temperature contours of the simulation results are shown in figs. 14 (for Model 1) and 15 (for Model 3), which give a clear illustration of how heat is being transmitted throughout the system. These contour plots help us analyze the patterns of heat distribution by making it simple to spot areas of high and low temperature. These models' visual representations make it easier to comprehend the system's overall thermal behavior.

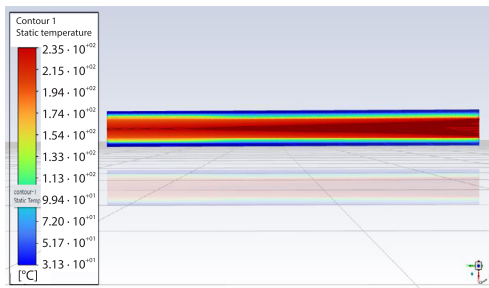


Figure 14. Temperature contour results of normal double pipe tube heat exchanger

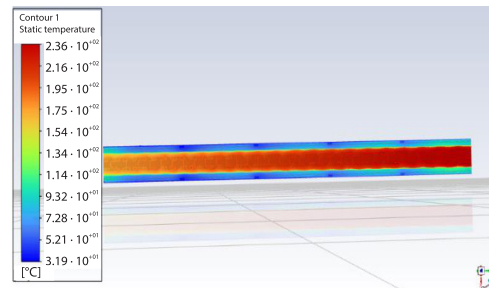


Figure 15. Temperature contour results of PFDPHE with alternate horizontal wing cut

Heat transfer rate

Figure 16 depicts the experimental findings for the DPHE rate of heat transfer based on eq. (10), and fig. 10 illustrates the results of the simulation. The results show that the finless normal tube heat exchanger produces the lowest rate of heat transfer. When the fin is attached on the outside of the inner tube, the rate of heat transmission dramatically rises. It makes sense that this inclination would increase the rate of heat transfer. It is thus impacted by the heat exchanger's rate of heat transfer. It is described that the maximum rate of heat transfer on experimentation is produced by the protracted finned tube heat exchanger with alternate horizontal wing cut. Considering the mean rate of heat transfer on experimental results, the protracted finned tube with alternate horizontal wing cut (Model 4) is 3.251 times better than the normal tube (Model 1), 1.159 times better than the protracted finned tube (Model 2) and 1.004 times better than the protracted tube with horizontal wing cut (Model 3). Figure 18 represents the mean heat transfer rate from the simulation, the protracted finned tube with alternate wing cut (Model 4) is 2.085 times better than the normal tube (Model 1), 1.286 times better than the protracted finned tube (Model 2) and 1.123 times better than the protracted finned tube with horizontal wing cut (Model 3).

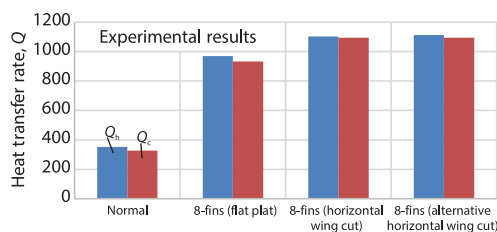


Figure 16. Heat transfer rate of experimentation results

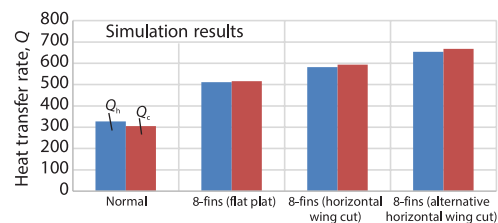


Figure 17. Heat transfer rate of simulation results

Coefficient of convective heat transfer

The convection heat transfer coefficients of exhaust gas in interaction with the inside surface of the inner tube for the investigated designs are based on eq. (8). The flow boundaries, such as fluid velocity and temperature differences, among others, have an consequence on the convective heat transfer coefficient. Larger convection coefficients were reached at higher fluid velocities and temperature differences. The fluid-flow passing throughout the heat exchanger has a tendency to develop turbulent with comparatively higher Reynolds numbers. One of the elements that affects the convection coefficient is turbulent flow. In experimentation, fig. 18, it was discovered that the maximum convective heat transfer coefficient happens on the protracted finned tube heat exchanger with alternate horizontal wing cut (Model 4) and it is 4.893 times better than normal tube (Model 1), 1.276 times better than the protracted tube (Model 2) and 1.009 times better than the protracted finned tube with horizontal wing cut (Model 3). In simulation results, fig. 19, it is illustrating that the maximum convective heat transfer coefficient happens on the protracted finned tube heat exchanger with alternate horizontal wing cut (Model 4) and it is 2.433 times better than normal tube (Model 1), 1.379 times better than the protracted tube (Model 2) and 1.164 times better than the protracted finned tube with horizontal wing cut (Model 3).

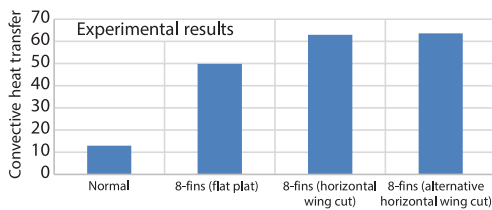


Figure 18. Convective heat transfer of experimentation results

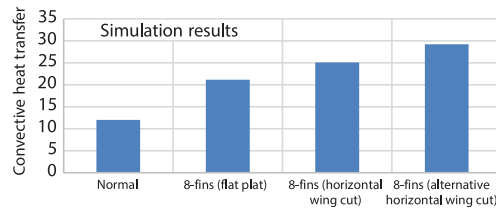


Figure 19. Convective heat transfer of simulation results

Effectiveness of the experimental and simulation are displayed in below fig. 20 based on eq. (2). It represents the ratio between the actual heat rate, q , and the maximum possible heat transfer rate, q_{max} , that can occur in a heat exchanger for a given set of fluids' conditions. Figure 20 represents the effectiveness difference between the experimental and simulation results.

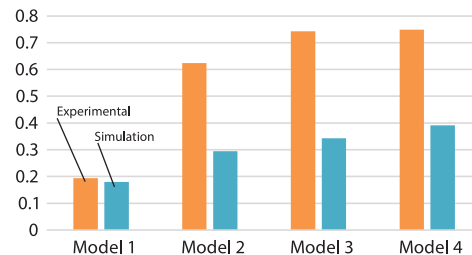


Figure 20. Effectiveness values of experimental and simulation results

Conclusions

A protracted finned DPHE is modelled in SolidWorks and analysed in ANSYS FLU-ENT in this study. This study aims to assess the heat transfer effects of the DPHE and optimise its design parameters for maximum performance. This experimental and simulation analysis has been performed by considering the protracted fin geometry on the internal tube of the heat exchanger set-up. The difference between the numerical simulation results and experimentation results, the percentage error on Model 1 (7%), Model 2 (49%), Model 3 (46%), and Model 4 (39%). Flat fins (Model 2), fins with a horizontal wing cut (Model 3), and fins with an alternate horizontal wing cut (Model 4) are the different fin geometries of the proposed heat exchanger design. The heat exchanger's effectiveness has been improved by adding fins to the inner tubes outside surface. These tendencies are influenced by the DPHE higher heat transfer area and

turbulence flow regime. Model 4 achieves higher heat transfer and coefficient of convective heat transfer, indicating a significant improvement in the performance of long-finned tube heat exchangers when modified with alternate horizontal wing cuts. The newly designed PFDPE with a 10 mm protrusion height has saved around 667 W of energy compared to the existing design with a 10 mm (30 mm) protrusion height, which saves 338 W (1014 W). The inclusion of a twisting tape insert within the inner tube makes the newly proposed design 1.97 times better than the existing design (base paper) by Ravi *et al.* [1].

In the future, more experimentation and simulation should be conducted to fully understand the complex physics of heat transfer in finned tubes. Further studies are needed to find newer geometries for more effective and efficient heat transfer designs that can be made by exploring the effects of higher turbulence in a fin-tube heat exchanger.

Nomenclature

A	– heat transfer area, [mm ²]	Q_{avg}	– average heat transfer rate, [W]
C	– specific heat capacity, [JKg ⁻¹ K ⁻¹]	Q_c	– heat transferred by cold fluid, [W]
C_{p_c}	– specific heat capacity of cold fluid, [JKg ⁻¹ K ⁻¹]	Q_h	– heat transferred by hot fluid, [W]
C_{p_h}	– specific heat capacity of hot fluid, [JKg ⁻¹ K ⁻¹]	Q	– heat transfer rate (q), [W]
C_{p_e}	– specific heat capacity exhaust gas, [JKg ⁻¹ K ⁻¹]	q	– heat transfer rate, [kW]
C_{p_w}	– specific heat capacity of cold water, [JKg ⁻¹ K ⁻¹]	Re	– Reynolds number
d_i	– inside diameter of inner tube, [mm]	T_{c_1}	– inlet temperature of cold fluid, [K]
d_o	– outside diameter of inner tube, [mm]	T_{c_2}	– outlet temperature of cold fluid, [K]
D_i	– inside diameter of outer tube, [mm]	T_{h_1}	– inlet temperature of hot fluid, [K]
D_o	– outside diameter of outer tube, [mm]	T_{h_2}	– outlet temperature of hot fluid, [K]
H_f	– protrusion height of fin, [mm]	ΔT	– change in temperature, [K]
h	– heat transfer coefficient, [Wm ⁻² K ⁻¹]	t	– thickness of pipe, [mm]
K_c	– thermal conductivity of cold fluid, [Wm ⁻¹ K ⁻¹]	t_f	– thickness of fin, [mm]
K_h	– thermal conductivity of hot fluid, [Wm ⁻¹ K ⁻¹]	Δt_c	– temperature difference of exhaust gas
L	– length, [mm]	Δt_w	– temperature difference of cold water
L_f	– total length of fin, [mm]	U	– overall coefficient of heat transfer, [Wm ⁻² K ⁻¹]
m	– mass-flow rate, [Kgs ⁻¹]	<i>Greek symbols</i>	
m_c	– mass-flow rate of cold fluid, [kgs ⁻¹]	η_{cold}	– thermal efficiency of hot cold
m_h	– mass-flow rate of hot fluid, [kgs ⁻¹]	η_{hot}	– thermal efficiency of hot fluid
m_e	– mass-flow rate of exhaust gas, [kgs ⁻¹]	η_{mean}	– mean thermal efficiency
m_w	– mass-flow rate of cold water, [kgs ⁻¹]	μ_c	– viscosity of cold fluid, [Nsm ⁻²]
Nu	– Nusselt number	μ_h	– viscosity of hot fluid, [Nsm ⁻²]
Pr	– Prandtl number	ρ_c	– density of cold fluid, [kgm ⁻³]
		ρ_h	– density of hot fluid, [kgm ⁻³]

References

- [1] Ravi, R., *et al.*, The CFD Analysis of Innovative Protracted Finned Counter Flow Heat Exchanger for Diesel Engine Exhaust Waste Heat Recovery, AIP Conference Proceedings, 2316 (2021), 030024
- [2] Baydaa, R. I., Aruna, K., Design and Analysis of Heat Exchanger, *International Journal of Scientific Engineering and Technology Research*, 03 (2014), 20, pp. 4181-4187
- [3] Moslem, Y., *et al.*, Optimum Waste Heat Recovery from Diesel Engines: Thermo-Economic Assessment of Nanofluid-Based Systems Using a Robust Evolutionary Approach, Proc. IMechE – Part E, *Journal Process Mechanical Engineering*, 233 (2019), 1, pp. 65-82
- [4] Chen, H., *et al.*, Experimental Investigation of Heat Transfer and Pressure Drop Characteristics of H-Type Finned Tube Banks, *Energies*, 7 (2014), 7, pp. 7094-7104
- [5] Zhu, D., *et al.*, Strategy on Performance Improvement of Inverse Brayton Cycle System for Energy Recovery in Turbocharged Diesel Engines, Proceedings of the Institution of Mechanical Engineers – Part A: *Journal of Power and Energy*, 234 (2020), 1, pp. 85-95
- [6] Amini, A., *et al.*, An Investigation Into the Use of The Heat Pipe Technology in Thermal Energy Storage Heat Exchangers, *Energy*, 136 (2017), Oct., pp. 163-172

- [7] Sai, C. P., et al., A Review on Optimization of Shell and Tube Heat Exchanger Used in Rankine Cycle of Exhaust Gas Waste Heat Recovery System, *International Journal of Scientific and Engineering Research*, 7 (2016), 6, pp. 185-193
- [8] Ravi, R., Pachamuthu, S., Design and Development of Innovative Protracted-Finned Counter Flow Heat Exchanger (PFCHE) for an Engine WHR and Its Impact on Exhaust Emissions, *Energies*, 11 (2018), 10, 2717
- [9] Aditya, L., Animesh, S., The CFD Investigation on Effective Utilization of Waste Heat Recovery from Diesel Engine Exhaust using Different Shaped Fin Protracted Heat Exchanger, *International Journal of Trend in Scientific Research and Development (IJTSRD)*, 4 (2020), 5, pp. 725-732
- [10] Reis, M. M. L., Gallo, W. L. R., Study of Waste Heat Recovery Potential and Optimization of the Power Production by an Organic Rankine Cycle in an FPSO Unit, *Energy Conversion and Management*, 157 (2018), Feb., pp. 409-422
- [11] Ram, T., et al., Design of Heat Exchanger for Waste Heat Recovery from Exhaust Gas of Diesel Engine, *Procedia Manufacturing*, 20 (2018), Jan., pp. 372-376
- [12] Fernandes, E. J., Krishanmurthy, S. H., Design and Analysis of Shell and Tube Heat Exchanger, *Int. J. Simul. Multidisci. Des. Optim.*, 13 (2022), 15, pp. 1-8
- [13] Modassir, T., Pathariya, A. K., Analysis of Plate Type Heat Exchanger with Substitute Pipe Arrangement using ANSYS, *International Journal of Advanced Research in Science, Communication and Technology (IJARSCT)*, 1 (2021), 1, pp. 4-16
- [14] Saidur, R., et al., Technologies to Recover Exhaust Heat from Internal Combustion Engines, *Renewable and Sustainable Energy Reviews*, 16 (2012), 8, pp. 5649-5659
- [15] Kim, T. K., et al., Experimental and Numerical Study of Waste Heat Recovery Characteristics of Direct Contact Thermoelectric Generator, *Energy Conversion and Management*, 140 (2017), May, pp. 273-280
- [16] Li, D., et al., Diesel Engine Waste Heat Recovery System Comprehensive Optimization Based on System and Heat Exchanger Simulation, *De Gruyter, Open Physics*, 19 (2021), 1, pp. 331-340
- [17] Ravi, R., et al., Computational and Experimental Investigation on Effective Utilization of Waste Heat from Diesel Engine Exhaust Using a fin Protracted Heat Exchanger, *Energy*, 200 (2020), 117489
- [18] Syuhada, A., et al., Heat Transfer Analysis on the Tube Type Heat Exchanger with Fin Pitch Variations, *IOP Conf. Series: Materials Science and Engineering*, 931 (2020), 012017
- [19] Cai, H., et al., Numerical and Experimental Study on the Influence of Top Bypass Flow on the Performance of Plate Fin Heat Exchanger, *Applied Thermal Engineering*, 146 (2019), Jan., pp. 356-363